

The r' -band luminosity function of Abell 1367: a comparison with Coma ^{*}

J. Iglesias-Páramo¹, A. Boselli¹, G. Gavazzi², L. Cortese², and J.M. Vílchez³

¹ Laboratoire d'Astrophysique de Marseille, BP8, Traverse du Siphon, F-13376 Marseille, France
e-mail: jorge.iglesias@astrsp-mrs.fr, alessandro.boselli@astrsp-mrs.fr

² Università degli Studi di Milano, Bicocca, Piazza delle Scienze, 3, 20126 Milano, Italy
e-mail: gavazzi@mib.infn.it, luca.cortese@mib.infn.it

³ Instituto de Astrofísica de Andalucía (CSIC), Apdo. 3004, 18080 Granada, Spain
e-mail: jvm@iaa.es

Received 4 June 2002; accepted 10 October 2002

Abstract. We made a large (approximately $1^\circ \times 1^\circ$) r' -band imaging survey of the central regions of the two nearby clusters of galaxies, Abell 1367 and Coma. The data, presented as a catalog, are used to construct the r' -band luminosity function (LF) of galaxies in these two clusters, by subtracting the Yasuda et al. (2001) galaxy counts from our cluster counts. Our Coma luminosity function is consistent with previous determinations, i.e. providing a faint end slope $\alpha = -1.47_{-0.09}^{+0.08}$, significantly steeper than the one we find for Abell 1367 ($\alpha = -1.07_{-0.16}^{+0.20}$). The counts in Abell 1367 show a relative minimum at $r' \approx 19$, followed by a steep increase faintward. The difference between the two clusters appears significant, given the consistency of the experimental conditions in the two clusters. Whereas for Coma we find a significant increase of the slope of the LF outwards, no such effect is found for Abell 1367.

Key words. atlases – galaxies: general – galaxies: clusters: general

1. Introduction

The study of the LF of galaxies provides us with a diagnostic tool indispensable for solving one of the hottest, yet unsettled cosmological issues, i.e. a plausible reconstruction of the evolution of galaxies from the epoch of their formation to the present. The comparison of the LF of galaxies in clusters and in the field, for example, should shed light on the role of the environment in regulating the evolution of galaxies, both for the giant and dwarf populations (see Press & Schechter 1974, Binggeli et al. 1988). Moreover the comparison of the galaxy LF in nearby clusters with that of clusters at progressively larger z can improve our knowledge of the evolution of galaxies in a given environmental condition. The recent work by Trentham & Tully (2002) on the LF in five different local environments up to $M_R = -10$, has shown that there are far fewer dwarfs than what expected from CDM models. The Coma cluster, being the prototype of evolved rich nearby clusters, is the one on which the attention has been most focused. After the catalogue of galaxies in the Coma

cluster (Godwin et al. 1983), several studies on this cluster have been published in different wavelength windows (e.g. Donas et al. 1991; Biviano et al. 1995; Lobo et al. 1997; Andreon 1999; Andreon & Pelló 2000). Considering the optical R -band alone, there is little agreement in the literature on the faint-end slope of the LF. The published values span from $\alpha \approx -1.20$ (Beijersbergen et al. 2002) to $\alpha \approx -1.7$ (Trentham 1998). Intermediate values of $\alpha \approx -1.30$ (Lugger 1989) and $\alpha \approx -1.40$ (López-Cruz et al. 1997; Bernstein et al. 1995; Secker 1997; Thompson & Gregory 1993) are also found. This remarkable lack of agreement is probably due to the inhomogeneity of the observational and data processing conditions, and different magnitude ranges or different cluster regions contributing to the determination of the LF.

Abell 1367, conversely, in spite of its many interesting structural aspects, has received little attention so far. After the first catalog of galaxies from Godwin & Peach (1982) very few studies have been carried out on the determination of the LF. Although Trentham (1997), attempted a LF in the R band, he could not perform a quantitative study of the LF because of the large uncertainties in the background subtraction. On the other hand Schechter (1976) and Kashikawa et al. (1995) presented fittings of the LF of Abell 1367 to analytical functions but

Send offprint requests to: J. Iglesias-Páramo

* Table 2 and catalogs described in Appendix are only available in electronic form at the CDS via anonymous ftp to cdsarc.u-strasbg.fr

they kept the parameter α fixed to -1.25 . Luger (1986) obtained a value of $\alpha = -1.42$ for the LF of Abell 1367 but his limiting magnitude was not deep enough to include the dwarf galaxies. In this work we present the r' -band LF of Abell 1367 that includes the dwarfs, and we compare it with the one of Coma, obtained under the same observational and instrumental conditions. Since both clusters have approximately the same recessional velocity (7000 and 6500 km sec $^{-1}$ respectively for Coma and Abell 1367), the limiting magnitudes as well as the selection biases are comparable. The differences between the two LFs, if any, should then be interpreted as due to the different evolutionary histories of the two clusters or to different initial conditions rather than to other observational or instrumental circumstances. A value of $H_0 = 75$ km s $^{-1}$ Mpc $^{-1}$ is adopted throughout this paper.

The paper is arranged as follows: Section 2 contains the details on the observations. Section 3 and 4 give details on the extraction of sources and the photometric calibration. Section 5 lists the different entries contained in the catalogs. Section 6 shows the LFs for both clusters and section 7 contains a brief summary and discussion of the results. A description of the catalogs is presented in Appendix A.

2. Observations

The data presented in this work are a by-product of an H α survey of nearby clusters aimed at constructing their H α LFs, whose main results can be found in Iglesias-Páramo et al. (2002). Observations were carried out with the Wide Field Camera (WFC) attached to the Prime Focus of the INT 2.5m located at Observatorio de El Roque de los Muchachos, on April 26th and 28th 2000, under photometric conditions, excepting the last half of the second night. However, since several exposures of each field were taken, we could properly calibrate all the data. The average seeing ranged from 1.5 to 2 arcsecs on both nights.

The WFC for the INT comprises a science array of four thinned AR coated EEV 4K \times 2K devices, plus a fifth acting as autoguider. The pixel scale at the detectors is 0.333 arcsec pixel $^{-1}$, which gives a total field of view of about 34 \times 34 arcmin 2 . Given the particular arrangement of the detectors, a squared area of about 11 \times 11 arcmin 2 is lost at the top right corner of the field. At the end, four fields covering a surface of about 1 $^\circ$ \times 1 $^\circ$ were observed (see Figure 2 in Iglesias-Páramo et al. 2002). The total exposure time for each field was 3 \times 300 s, except for one field in Coma for which a single 300 s exposure was taken.

No broad band photometric standards were observed since the observational run was not devoted to produce broad band catalogs. However, relative calibration between the different frames were possible given that spectrophotometric standards for H α calibration were observed. Detailed information about the observations and data reduction procedure can be found in Iglesias-Páramo et al. (2002).

3. Extraction of Sources

The identification and extraction of sources was carried out using the code *SExtractor* (see Bertin & Arnouts 1996, for details). The limiting size and limiting flux for detection of objects were set to 49 pixels (which corresponds approximately to the size of the seeing disk in the frames) and 2.5 times the standard deviation of the sky, respectively, in order to minimize the number of spurious detections.

The regions corresponding to the wings of the PSF of bright, saturated stars were removed. The separation between stars and galaxies is based on the G/S parameter, ρ , given by *SExtractor* (see Bertin & Arnouts 1996). To the first approximation, we accept as galaxies all objects with $\rho < 0.05$, and stars those with $\rho > 0.95$. For the rest of the objects, a closer inspection based on the FWHM estimated by the IMEXAM task running on IRAF¹ was performed and those which were undoubtedly found to be stars were removed. We point out the possibility of losing compact galaxies that are unresolved in our CCD frames in the process of rejecting stars as suggested by Andreon & Cuillandre (2002). In order to test whether a population of compact dwarf galaxies was lost in the inner parts of the clusters, we performed counts of our rejected unresolved objects with magnitudes in the range $-18 \leq R_C \leq -15$ ² over the inner disk $D \leq 0.4$ degrees and the outer annulus $D \geq 0.5$ degrees. Surprisingly we found an excess of counts per squared degree in the outer annulus for Abell 1367 whereas for Coma the excess of counts per squared degree was found in the inner disk. Thus, no conclusive results of a systematic loss of compact galaxies can be stated from our data.

An astrometric solution was found with the USNO³ catalog of stars for each individual frame. After checking the rms of the fitting and the absolute offsets between the coordinates found for those objects appearing in more than one frame, the accuracy of this solution was found to be approximately 2 arcsecs.

A total of 149 galaxies common to more than one frame was removed by direct inspection. When multiple detections existed for an object, we ruled out the one presenting the worst quality. The criteria to decide the quality of the detections include the distance to the border of the frame, the existence of halos of diffuse light from bright stars and the vignetting of the North part in detector #3. The measured photometry for the multiple objects was also used to obtain the relative calibration between the different detectors.

¹ IRAF is distributed by the National Optical Astronomy Observatories, which are operated by the Association of Universities for Research in Astronomy, Inc., under cooperative agreement with the National Science Foundation.

² this is the range of magnitudes found for the BCDs

³ United States Naval Observatory

4. Photometry

The final instrumental magnitudes are derived using *SExtractor's* MAG_BEST magnitudes. A total magnitude is provided for the galaxies following Kron's (1980) first moment algorithm. However for those galaxies suspected to have a neighbor biasing the magnitude by more than 0.1 mag, a corrected isophotal magnitude is provided (see Bertin & Arnouts 1996 for more details). For the objects for which the corrected isophotal magnitude was obtained, we compared it with that computed by performing detailed aperture photometry. In Table 1 we show the fraction of galaxies for which our aperture magnitude differs by more than 0.2 magnitude from the magnitude provided by *SExtractor*, in three magnitude intervals. Even for most of the faintest galaxies, the *SExtractor's* magnitudes agree with our more accurate aperture magnitudes within 20%, which is accurate enough for a statistical analysis of the LF.

The instrumental zero point was first estimated from the $H\alpha$ calibration, taking into account the airmass, the relative calibration between the different detectors and the scaling factor between the broad band and the $H\alpha$ frames, which were taken respectively with a Sloan-Gunn r' and a narrow band [SII] filters (see Iglesias-Páramo et al. 2002 for details on the instrumental setup). This provided us with instrumental magnitudes already corrected for airmass and for chip-to-chip variation, that could be directly compared with the published photometry.

The procedure used for the calibration of our data is the following: we searched in the literature for all galaxies belonging to any of the two clusters with available aperture photometry in any photometric band with an effective wavelength close to 6000 Å, namely R Cousins, r Gunn and r' Sloan. The relationship between our instrumental magnitudes (M_{ins}) and the ones corresponding to the different photometric systems at similar effective wavelengths are:

$$R_{Cousins} = m_{ins} + Z_{Cousins} \quad (1)$$

$$r_{Gunn} = m_{ins} + Z_{Gunn} \quad (2)$$

$$r'_{SDSS} = m_{ins} + Z_{SDSS} \quad (3)$$

respectively for the Cousins, Gunn and Sloan photometric systems.

Expected values for the differential zero points are

$$Z_{Gunn} - Z_{Cousins} = 0.35 \quad (4)$$

and

$$Z_{Gunn} - Z_{SDSS} = 0.15 \quad (5)$$

from Jorgensen (1994) and Fukugita et al. (1996).

We did not apply a color correction because of the lack of any color information for the target galaxies. Given the similarity of the filter profiles (λ_{eff} , $\Delta\lambda$) in the three photometric systems mentioned above, we expect an almost negligible color term in the conversion equations,

thus our instrumental magnitudes can be converted to any of the three systems (see Fukugita et al. 1995 for details on the color effects for the different galaxy types in different photometric systems). Furthermore, if any color term is present, it would be negligible compared to the bin width used in the construction of the LF ($\Delta r' = 0.5$ mag), thus unaffacting the main results of the present study.

Jorgensen et al. (1992) give Gunn r -band aperture photometry for a large sample of ellipticals and S0s belonging to the Coma cluster. We performed instrumental photometry of the galaxies in common using the same apertures. For cross-calibration we used the galaxies with intermediate magnitudes (in the range $14.0 \leq r' \leq 16.0$). The faintest galaxies were excluded because they have the largest statistical errors. Marin-Franch & Aparicio (2002) performed Cousins R_C -band aperture photometry for a sample of galaxies in the central regions of Coma. Their data were taken at the 2.5m INT, with the same instrumental configuration as ours. They made aperture photometry of eight galaxies in common with our catalog.

Figure 1 shows the difference between our instrumental magnitudes and the published magnitudes vs. the R_C magnitudes. The horizontal lines show the median value of the distributions. The best fitting results for the zero points expressed in Cousins R magnitudes are $Z_{Gunn} = -28.90 \pm 0.15$ (for the data of Jorgensen et al. 1992) and $Z_{Cousins} = -29.27 \pm 0.09$ (for the data of Marin-Franch & Aparicio 2002).

After correlating both independent calibrations, we obtained $Z_{Gunn} - Z_{Cousins} = 0.37$, which is in good agreement with the expected value for these two photometric systems (Eq. 4). For Abell 1367 we adopt the same value of $Z_{Cousins}$ since the night was photometric and the same instrumental setup was used.

In addition we applied average corrections for Galactic extinction following Schlegel et al. (1998), that amounts to 0.02 and 0.06 mag for Coma and Abell 1367 respectively.

In what follows, we will refer our photometry to the Sloan r' -band system for convenience (since the used background counts are refereed to this system, see section 6 for more details) using Eqs. 1 to 3.

5. The Catalogs

Two catalogs are produced containing 4413 and 5555 galaxies respectively for Abell 1367 and Coma. Both are available electronically from the CDS site. A one-page sample of the catalogs is given in appendix A. The catalogs are arranged as follows:

- (1): Name of the object.
- (2)-(7): Right Ascension and Declination (J2000), with an accuracy of $\approx 2''$.
- (8): Sloan r' -band magnitude following the Kron method.
- (9): Error in the Sloan r' -band magnitude, provided by *SExtractor*.
- (10): Surface brightness within the Sloan r' 25.5 mag arcsec $^{-2}$ isophote.
- (11): Error in the surface brightness within the Sloan r'

25.5 mag arcsec $^{-2}$ isophote estimated as the inverse of the signal to noise of the galaxies within the area enclosed by the 25.5 mag arcsec $^{-2}$ isophote.

(12): Area of the r' 25.5 mag arcsec $^{-2}$ isophote in arcsec 2 .

(13): Number in the catalogs Godwin & Peach (1982, for Abell 1367) and Godwin et al. (1983, for Coma). 0 indicates galaxies without an identification in the Godwin's catalogs.

(14): Position angle of the elliptical profile, north to east (in degrees).

(15): Ellipticity ($1 - b/a$, where a and b are respectively the major and minor axis of the elliptical profile).

(16): Star-Galaxy separator (Close to 0 means galaxy-like, close to 1 means star-like).

Figure 2 shows the Sloan r' -band total galaxy counts for both clusters. Error bars contain only the poissonian term. As can be seen from the figure, the limiting magnitude for both clusters is around 21 mag. However, given the shorter exposure time for one of the fields in Coma, we adopt a conservative 20.5 mag completeness limit of our survey.

6. The Luminosity Functions

The membership of galaxies to the two studied clusters is known from complete redshift measurements only down to 15.5 (Abell 1367) and 16.5 (Coma) magnitudes. Thus, to construct the r' -band LFs some statistical subtraction is necessary in order to decontaminate our catalogs from background and foreground galaxies. Since the aim of our observations was to construct the H α LF and not the r' LF, we have not taken observations of a reference field from which the galaxy counts could be estimated. Thus, to perform the statistical subtraction of background galaxies we must rely on galaxy counts taken from the literature. Various sets of galaxy counts from different sources in the literature exist for similar effective wavelengths. Figure 3 shows galaxy counts transformed to the Sloan r' -band system for several sources in the literature (Koo 1986; Metcalfe et al. 1991; Yasuda et al. 2001; Paolillo et al. 2001; Beijersbergen et al. 2002). A large dispersion exists between the different galaxy counts sets. We also added for comparison the galaxy counts from the most external fields of Abell 1367 (i.e. detectors #2 and #3 of exposure 1; see Figure 2, left panel in Iglesias-Páramo et al. 2002 for more clarity). Given that these two exposures are about 1° far from the cluster center, the contamination due to the cluster galaxies should be almost negligible. Thus, the counts from these frames should be reasonably similar to the true background galaxy counts. As it is apparent in the zoomed right panel of Figure 3, the galaxy counts from the SDSS match reasonably well our external counts for Abell 1367 towards faint magnitudes. We select this set of galaxy counts in order to decontaminate our cluster counts for the background and foreground population. We stress the fact that the results obtained for the LF will depend on the background counts used to decon-

taminate the total counts. The uncertainty in the galaxy counts due to the cosmic variance of the background is taken into account in the error budget as it is explained below.

There is a further concern about the subtraction of the background counts related to the fact that both the Abell 1367 and Coma clusters belong to the Great Wall (see Ramella et al. 1992). Whether the Great Wall should be considered as a background source for the two clusters is a matter of debate. Gavazzi et al. (1995) applied a caustic model to determine the membership to the clusters. As can be seen from their Figure 7, almost all galaxies with radial velocities within 3σ of the average velocity of any of the two clusters and within the range of projected radial distances covered by our survey are considered as members of the clusters. This suggests that the contamination by supercluster members is non important at least within the area covered by our data. Thus, we decided not to apply any correction due to supercluster population. We remark however that the analysis by G95 was based on galaxies from the Zwicky catalog, and nothing can be said about the dwarf galaxies.

A further point concerning the construction of a proper LF is the normalization of the galaxy counts to the same area. The total area covered by our mosaic of detectors is 1.07 and 1.03 $^{\circ 2}$ for Abell 1367 and Coma respectively. However, after correction for the area lost because of the presence of strongly saturated stars, the gaps between chips and the vignetting at the upper left corner of detector #3, the effective covered area is 0.97 $^{\circ 2}$ for both clusters.

In order to account for all the possible sources of error (see Huang et al. 1997), we included the contributions from the cosmic variance of the background counts (this contribution was added twice, to the cluster counts and to the background counts as suggested by Andreon & Cuillandre 2002), the contribution corresponding to the photometric error of the zero point and the poissonian term.

After subtraction of the background galaxy counts, we fitted the resultant points with the Schechter functional form (Schechter 1976):

$$\phi(m_{r'}) = \phi^* \times [10^{0.4(m^* - m_{r'})}]^{\alpha+1} e^{-10^{0.4(m^* - m_{r'})}} \quad (6)$$

The fitting procedure used minimizes the χ^2 and takes into account the errors and assigns to each bin a statistical weight equal to $1/\sigma_i^2$, where σ_i is the error term corresponding to bin i .

The value of the parameter α is of special relevance for our study because it accounts for the relative dwarf-to-giant populations of galaxies in the clusters.

6.1. Coma: Comparison with Previous Studies

As a starting point, we will compare the total counts in the Coma cluster with others already existing in the literature. For this purpose we selected the compilations by Bernstein

et al. (1995), Trentham (1998), Beijersbergen et al. (2002) and Andreon & Cuillandre (2002). All these works present R_C -band data on the Coma cluster over regions of the sky totally or partially covered by our survey. The comparison between our total counts and the ones mentioned above, restricted to a common region, are presented in Figure 4. Our limiting magnitude, $M_{r'} = -14.32$, is marked with a vertical dashed line.

Bernstein et al. (1995) obtained very deep R_C -band CCD imaging of a small field close to the X-ray center of the cluster, covering an area of $7.5'$ square (covered by our survey). The two sets of data are consistent within 1σ up to our limiting magnitude.

Trentham (1998) obtained data in a small region (approximately $0.18 \text{ }^{\circ 2}$, covered by our survey) in the R_C -band. The agreement between the two sets of data is very good. The slight (within 1σ) discordance at $M_R \approx -15$ mag could be due to the different method used to extract the objects: *SExtractor* in this work and FOCAS in Trentham's paper.

Beijersbergen et al. (2002) presented data taken with the WFC at the INT as ours. Although the area covered by their survey is larger than ours, they also presented the LF for the inner region of the cluster which was also covered by us. All points are consistent within 1σ in the range of completeness of our data.

We finally compare our data with those of Andreon & Cuillandre (2002). These authors present a very deep survey of the central part of the Coma cluster in three bands: B , V and R . In this case, the region of the sky covered by these authors did not exactly match with ours, but the two areas overlap by 90% of their total surveyed area. The data of Andreon & Cuillandre are normalized to ours at $R_C = 18$. Once again, the data are consistent within our magnitude range of completeness.

The comparison with four independent sources in the literature shows that our data are consistent within 1σ with all of them. Any residual difference in the derived LF should depend purely on the adopted background counts, on the effective surveyed area and on the range of magnitudes over which the LF is computed.

Figure 5 shows our LF for the total area covered in the Coma cluster for $r' = 20.5$ mag, assuming the background counts selected in the previous section. The values of the best fitting Schechter parameters are $\phi^* = 21.83 \pm 7.36$, $\alpha = -1.47_{-0.09}^{+0.08}$, and $M_{r'}^* = -21.63_{-0.57}^{+0.46}$ with $\chi_\nu^2 = 1.69$. As previously claimed, we find that a Schechter function is not the best representation of the Coma LF in the area covered by our survey. Most of the points show deviations by more than 1σ from the best fitting function. The distribution shows two local minima around $M_{r'} \approx -19$ and -17 which significantly deviate from the fit at the 1σ level. There is also a maximum centered at $M_{r'} \approx -20.5$ with four points not fitting the Schechter fit.

In order to make a better estimate of the faint end slope of the LF, we fit our data to an exponential function of the type $\approx 10^{km}$ where m is the absolute magnitude

and the constant k is related to the α parameter of the Schechter function by the relation:

$$\alpha = -(k/0.4 + 1) \quad (7)$$

The best fitting is shown in Figure 5 with a dotted line. The best fitting slope is $k = 0.22 \pm 0.03$ with $\chi_\nu^2 = 0.77$ in the magnitude range $-19 \leq M_{r'} \leq -14.5$ (corresponding to $\alpha = -1.55$).

6.2. Abell 1367

Figure 6 shows our LF for the total area covered in Abell 1367 in the magnitude range of completeness ($M_{r'} \leq -14.19$). The best fitting Schechter parameters are $\phi^* = 35.66 \pm 12.40$, $\alpha = -1.07_{-0.16}^{+0.20}$, and $M_{r'}^* = -21.20_{-0.63}^{+0.60}$ with $\chi_\nu^2 = 0.53$. In this case, the Schechter function provides a good fitting of the data except for 3 points which do not fit the model within 1σ . The errors become very large for $M_{r'} \geq -17$. We also fit an exponential function over the same range of magnitudes as for the Coma LF and obtain a value for the slope of $k = 0.02 \pm 0.06$, corresponding to $\alpha = -1.05$, with $\chi_\nu^2 = 0.66$.

The comparison of the LFs of Coma and Abell 1367 is shown in Figure 6 (the shaded band corresponding to the uncertainty region of Coma LF). As can be seen from the plot, at most of the magnitudes, LFs of both clusters do not coincide at the 1σ level. This effect is mostly due to the different richness of both clusters. However, the shapes of the LFs also show appreciable differences: The LF of Abell 1367 does not show the bump at $M_{r'} \approx -20$ exhibited by the Coma LF. The steep rise of the slope of the Abell 1367 LF in the interval $-15.5 \leq r' \leq -14.5$ cannot be trusted due to large statistical uncertainties.

Figure 7 shows the 1 , 2 and 3σ confidence contours for the best fitting Schechter function parameters of both clusters. Although the errors in the determination of the parameters of the Abell 1367 LF are large, even the 3σ contours do not cross each other, supporting the conclusion that the slopes of the two clusters are significantly different at this level.

The ratio of dwarf-to-giant galaxies is considerably higher in Coma than in Abell 1367. This result, together with the fact that the H α LFs of both clusters are fairly similar (Iglesias-Páramo et al. 2002), indicates that an important population of non star-forming dwarf galaxies present in Coma is absent in Abell 1367.

6.3. The Influence of the Cluster Environment on the LFs of Coma and Abell 1367

Beijersbergen et al. (2002) found that the faint end of the LF of the Coma cluster steepens as we move outwards in the cluster. We repeat a similar exercise for the two studied clusters. In order to minimize errors due to the limited statistics (mostly severe for the outer parts of Abell 1367), we select only two regions of each cluster: an inner one of radius 0.4° and an external one with projected radius larger than 0.5° . Galaxies belonging to the

annulus $0.4^\circ < R < 0.5^\circ$ are excluded from this analysis. The cluster centers were assumed coincident with the peak of the extended X-ray sources (Donnelly et al. 1998 for Abell 1367; White et al. 1993 for Coma). We use the same radius for both clusters because not only are they at approximately the same distance, but also the estimates of their physical sizes coincide (see Girardi et al. 1995). The virial radii were estimated as 0.5° and 0.4° and the core radii as 0.12° and 0.08° respectively for Abell 1367 and Coma.

Figure 8 shows the LFs of the two clusters restricted to the two regions mentioned above. The data are binned by 1 mag in order to increase the statistics, and fitted to exponential functions. As can be seen in the left panel of Figure 8 the slopes of the LFs of the two regions of Coma are clearly different from each other. The best fit values for the slopes over the range $-19 \leq M_r \leq -14.5$ are $k_{in} = 0.19 \pm 0.03$ and $k_{out} = 0.34 \pm 0.07$ for the inner and outer regions respectively.

For Abell 1367 the restricted LFs are shown in the right panel of the same figure. The cluster counts become negative at $M_{r'} \approx -15.5$ for the external annulus and the error bars are very large fainter than $M_{r'} = -16.5$ affecting the reliability of this comparison. The slopes obtained from the best fitting to the exponential function (in the same magnitude range as for Coma) are $k_{in} = 0.06 \pm 0.06$ and $k_{out} = 0.09 \pm 0.11$ for the inner and outer regions respectively, thus showing consistency. However, we stress that the slope for the outer annulus was computed rejecting the negative point at $M_{r'} \approx -15.5$, and that the real uncertainty could be even larger than the one obtained from the least squared fitting.

7. Summary and Conclusions

We present new deep catalogs containing positions and r' -band photometry of galaxies in the central $1^\circ \times 1^\circ$ of the nearby clusters Abell 1367 and Coma. These catalogs are used to determine the SDSS r' -band LFs of both clusters by subtracting the Yasuda et al. (2001) galaxy counts from our cluster counts. The faint-end slope of the Coma LF is $\alpha = -1.47_{-0.09}^{+0.08}$ whereas that of the Abell 1367 LF is shallower, with $\alpha = -1.07_{-0.16}^{+0.20}$. This difference is found significant at the 3σ level. Given that the observations of both clusters were obtained in homogeneous conditions, we argue that these differences are not due to instrumental or data handling biases, but they are intrinsic to the clusters. We also stress that the differences are not due to the background counts since the best set of galaxy counts was used to decontaminate the counts of both clusters.

The LF parameters strongly depend on the surveyed region, on the background counts used to decontaminate the cluster counts and on the magnitude range over which the fitting is performed. Other determinations of the LFs of the same clusters (in section 6.1 we checked that our total Coma counts are consistent with several sources in the literature), is valid only with those covering a similar area and with substantial overlapping.

Concerning the comparison with the LF of field galaxies, the values of α derived for Coma and Abell 1367 are consistent with those of the field, which show a larger spread of parameters: Lin et al. (1996) found $\alpha = -0.70 \pm 0.05$ ($M_R < -17.5$), Geller et al. (1997) found $\alpha = -1.17 \pm 0.19$ ($M_R < -16$) and Blanton et al. (2001) reported $\alpha = -1.20 \pm 0.03$ ($M_{r'} < -16$).

The slope of the LF of Coma is found steeper towards the cluster outskirts within 1σ statistical significance. No such trend is observed in Abell 1367. This means that the bright-to-faint galaxy ratio in Coma decreases as we move outwards the cluster. The observed increase of α in the cluster's outskirts could be explained both by an increase of the dwarf population or by a decrease of the giant population with respect to the cluster center. It would be interesting to find out at which clustercentric distance the cluster LF would approach the one of the field. Once again Coma and Abell 1367 would be the ideal clusters to do this test: they are both embedded in the Great Wall (Geller & Huchra 1990) located at the same distance of ~ 6500 – 7000 km s^{-1} . A survey of some square degrees in between the two clusters would suffice to map the variations of the LF with increasing clustercentric distances. Given the low density of supercluster galaxies, a deep redshift survey is however needed.

Acknowledgements. We thank S. Andreon for his interesting comments and suggestions. This research has made use of the NASA/IPAC Extragalactic Database (NED) which is operated by the Jet Propulsion Laboratory, California Institute of Technology, under contract with the National Aeronautics and Space Administration. The INT is operated on the island of La Palma by the ING group, in the Spanish Observatorio del Roque de Los Muchachos of the Instituto de Astrofísica de Canarias. JIP acknowledges the Fifth Framework Program of the EU for a Marie Curie Postdoctoral Fellowship.

References

- Andreon, S. 1999, A.& A., 351, 65
- Andreon, S. & Pelló, R. 2000, A.& A., 353, 479
- Andreon, S. & Cuillandre, J.-C. 2002, Ap.J., 569, 144
- Beijersbergen, M., Hoekstra, H., van Dokkum, P. G., & van der Hulst, T. 2002, M.N.R.A.S., 329, 385
- Bernstein, G. M., Nichol, R. C., Tyson, J. A., Ulmer, M. P., & Wittman, D. 1995, A.J., 110, 1507
- Bertin, E. & Arnouts, S. 1996, A.& A.S., 117, 393
- Binggeli, B., Sandage, A., & Tammann, G. A. 1988, A.R.A.& A., 26, 509
- Biviano, A., Durret, F., Gerbal, D., Le Fevre, O., Lobo, C., Mazure, A., & Slezak, E. 1995, A.& A., 297, 610
- Blanton, M. R. et al. 2001, A.J., 121, 2358
- Donas, J., Milliard, B., & Laget, M. 1991, A.& A., 252, 487
- Donnelly, R. H., Markevitch, M., Forman, W., Jones, C., David, L. P., Churazov, E., & Gilfanov, M. 1998, Ap.J., 500, 138
- Fukugita, M., Shimasaku, K., & Ichikawa, T. 1995, P.A.S.P., 107, 945
- Fukugita, M., Ichikawa, T., Gunn, J. E., Doi, M., Shimasaku, K., & Schneider, D. P. 1996, A.J., 111, 1748
- Gavazzi, G., Randone, I., & Branchini, E. 1995, Ap.J., 438, 590

- Geller, M. & Huchra, J. 1990, *Scientific American*, 262, 19
- Geller, M. J. et al. 1997, *A.J.*, 114, 2205
- Girardi, M., Biviano, A., Giuricin, G., Mardirossian, F., & Mezzetti, M. 1995, *Ap.J.*, 438, 527
- Godwin, J. G. & Peach, J. V. 1982, *M.N.R.A.S.*, 200, 733
- Godwin, J. G., Metcalfe, N., & Peach, J. V. 1983, *M.N.R.A.S.*, 202, 113
- Huang, J.-S., Cowie, L. L., Gardner, J. P., Hu, E. M., Songaila, A., & Wainscoat, R. J. 1997, *Ap.J.*, 476, 12
- Iglesias-Páramo J., Boselli A., Cortese L., Vílchez J.M., Gavazzi G., 2002, *A.& A.*, 384, 383
- Jorgensen, I., Franx, M., & Kjaergaard, P. 1992, *A.& A.S.*, 95, 489
- Jorgensen, I. 1994, *P.A.S.P.*, 106, 967
- Kashikawa, N., Shimasaku, K., Yagi, M., Yasuda, N., Doi, M., Okamura, S., & Sekiguchi, M. 1995, *Ap.J.*, 452, L99
- Koo, D. C. 1986, *Ap.J.*, 311, 651
- Kron, R. G. 1980, *Ap.J.S.*, 43, 305
- Lin, H., Kirshner, R. P., Sheckman, S. A., Landy, S. D., Oemler, A., Tucker, D. L., & Schechter, P. L. 1996, *Ap.J.*, 464, 60
- Lobo, C., Biviano, A., Durret, F., Gerbal, D., Le Fevre, O., Mazure, A., & Slezak, E. 1997, *A.& A.*, 317, 385
- Lopez-Cruz, O., Yee, H. K. C., Brown, J. P., Jones, C., & Forman, W. 1997, *Ap.J.*, 475, L97
- Lugger, P. M. 1986, *Ap.J.*, 303, 535
- Lugger, P. M. 1989, *Ap.J.*, 343, 572
- Marin-Franch, A., & Aparicio, A. 2002, *Ap.J.*, 568, 174
- Metcalfe, N., Shanks, T., Fong, R., & Jones, L. R. 1991, *M.N.R.A.S.*, 249, 498
- Paolillo, M. et al. 2001, *A.& A.*, 367, 59
- Press, W. H. & Schechter, P. 1974, *Ap.J.*, 187, 425
- Ramella, M., Geller, M. J., & Huchra, J. P. 1992, *Ap.J.*, 384, 396
- Schechter, P. 1976, *Ap.J.*, 203, 297
- Schlegel, D. J., Finkbeiner, D. P., & Davis, M. 1998, *Ap.J.*, 500, 525
- Secker, J., Harris, W. E., & Plummer, J. D. 1997, *P.A.S.P.*, 109, 1377
- Thompson, L. A. & Gregory, S. A. 1993, *A.J.*, 106, 2197
- Trentham, N. 1997, *M.N.R.A.S.*, 290, 334
- Trentham, N. 1998, *M.N.R.A.S.*, 293, 71
- Trentham, N. & Tully, R.B. 2002, *astro-ph/0205060*
- White, S. D. M., Briel, U. G., & Henry, J. P. 1993, *M.N.R.A.S.*, 261, L8
- Yasuda, N. et al. 2001, *A.J.*, 122, 1104

Table 1. Percentage of galaxies for which $|r'_{Aper} - r'_{Sex}| > 0.2$, for different magnitude intervals.

Magnitude Interval	Fraction (%)
$15.5 \leq r' < 17.5$	0.9
$17.5 \leq r' < 19.5$	2.9
$19.5 \leq r' < 21.0$	8.6

Table 2. Number counts and errors for both clusters and the background counts in the SDSS photometric system (Sloan r' -band magnitudes). To be published electronically.

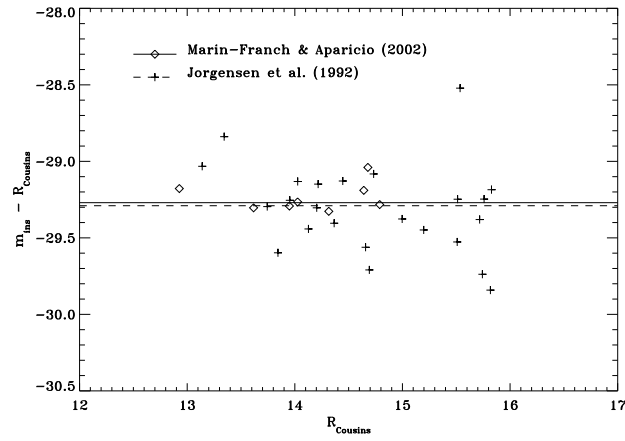


Fig. 1. R magnitude vs. the difference between our instrumental magnitudes and R -band magnitudes from Jorgensen et al. (1992, crosses) and Marin-Franch & Aparicio (2002, open diamonds). Both sets of data are expressed in Cousins R magnitudes. The horizontal lines represent the median values of both distributions.

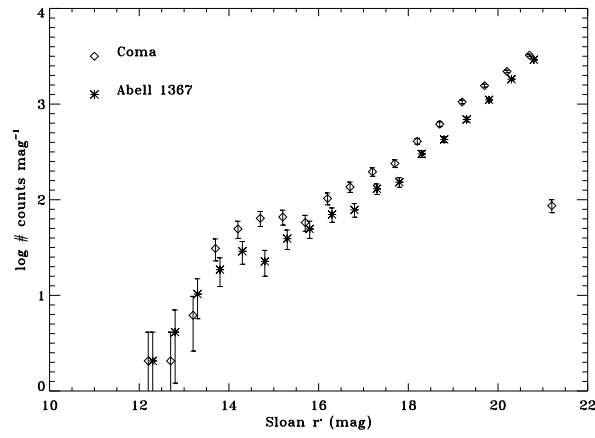


Fig. 2. Galaxy counts in the Sloan r' -band for Abell 1367 (asterisks) and Coma (open diamonds). Error bars include Poisson errors. The abscissas have been shifted $+0.05$ and -0.05 magnitudes respectively for Abell 1367 and Coma, avoiding superposition of points.

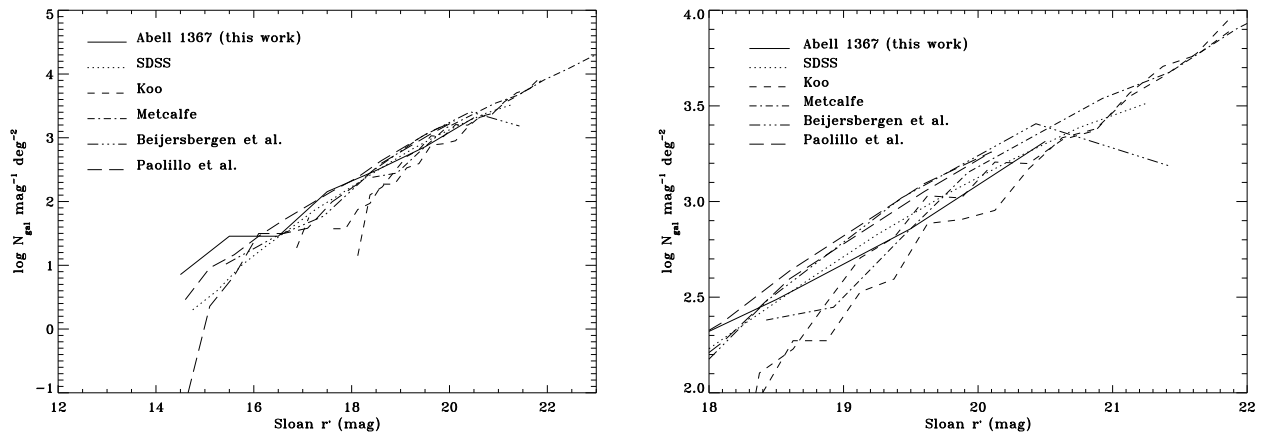


Fig. 3. **Left panel:** Sloan r' -band galaxy counts from several sources extracted from the literature. **Right panel:** Same as left panel zoomed at the faint magnitude end of the distribution.

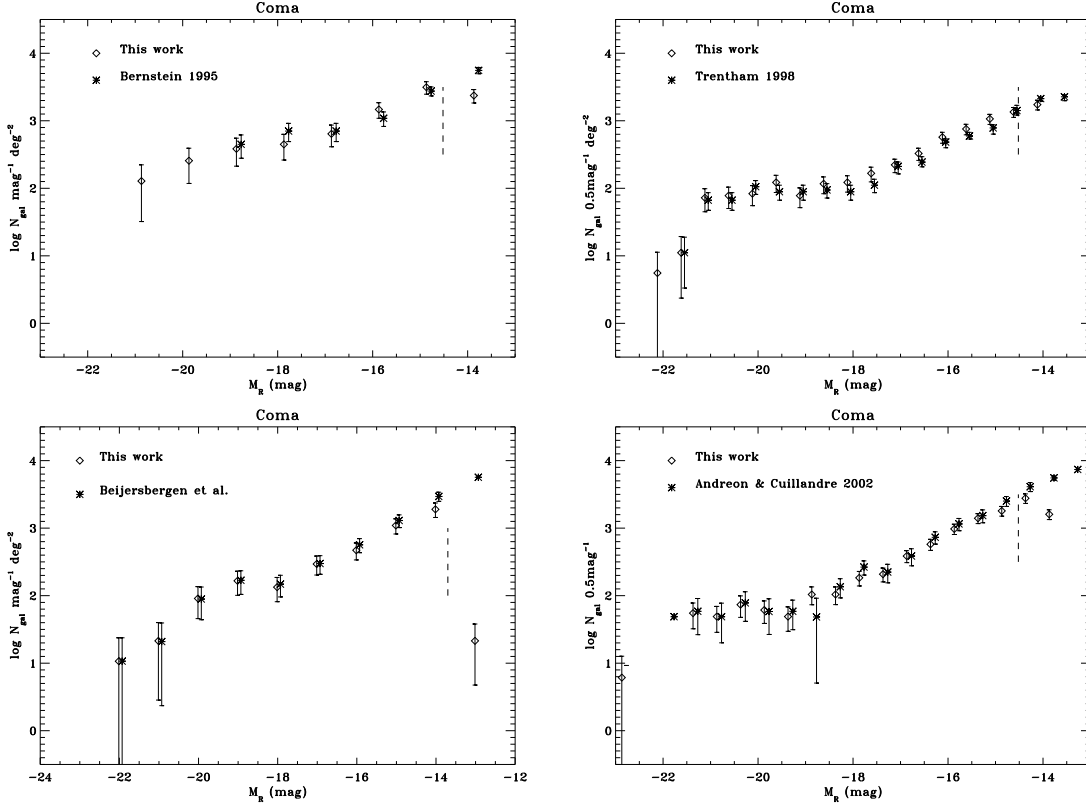


Fig. 4. Comparison of our galaxy counts prior to background subtraction for Coma with those of Bernstein et al. (1995), Trentham et al. (1998), Beijersbergen et al. (2002) and Andreon & Cuillandre (2002). At each plot, both sets of counts are referred to the same region of the sky. The dashed vertical line indicates our adopted limiting magnitude in the R_C -band. The abscissas corresponding to our data and other author's are shifted by $+0.05$ and -0.05 mag respectively for clarity.

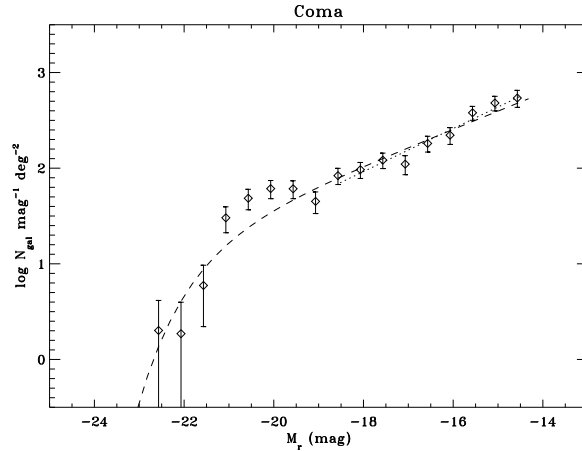


Fig. 5. Sloan r' -band LF for Coma in the range of completeness of the data ($M_{r'} \leq -14.32$). Error bars include the cosmic variance, the zero point and the poissonian error terms for both the total counts and the background counts. The best fitting Schechter function is indicated with a dashed line. The best fitting exponential function in the range $-19 \leq M_{r'} \leq -14.5$ is indicated with a dotted line.

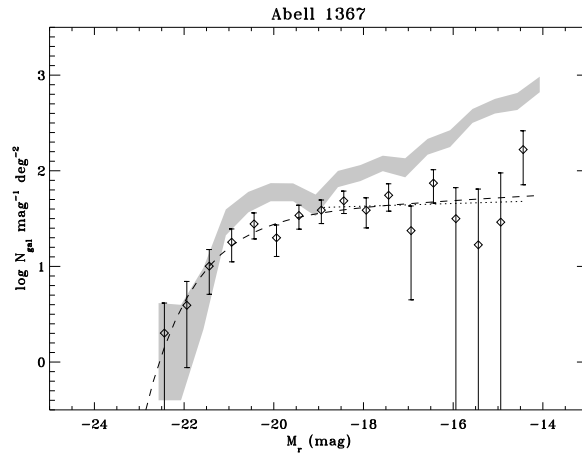


Fig. 6. Sloan r' -band LF for Abell 1367 in the range of completeness of the data ($M_{r'} \leq -14.19$). Error bars include the same terms as in Figure 5. The dashed line indicates the best fitting to a Schechter function. The dotted line corresponds to the best fitting to an exponential function in the range $-19 \leq M_{r'} \leq -14.5$. The shaded region is the Coma LF within its 1σ error bars.

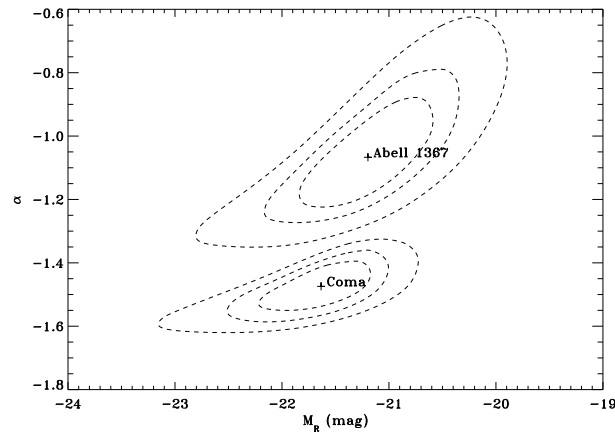


Fig. 7. 1, 2 and 3σ confidence contours for the best fitting Schechter function parameters of Abell 1367 and Coma.

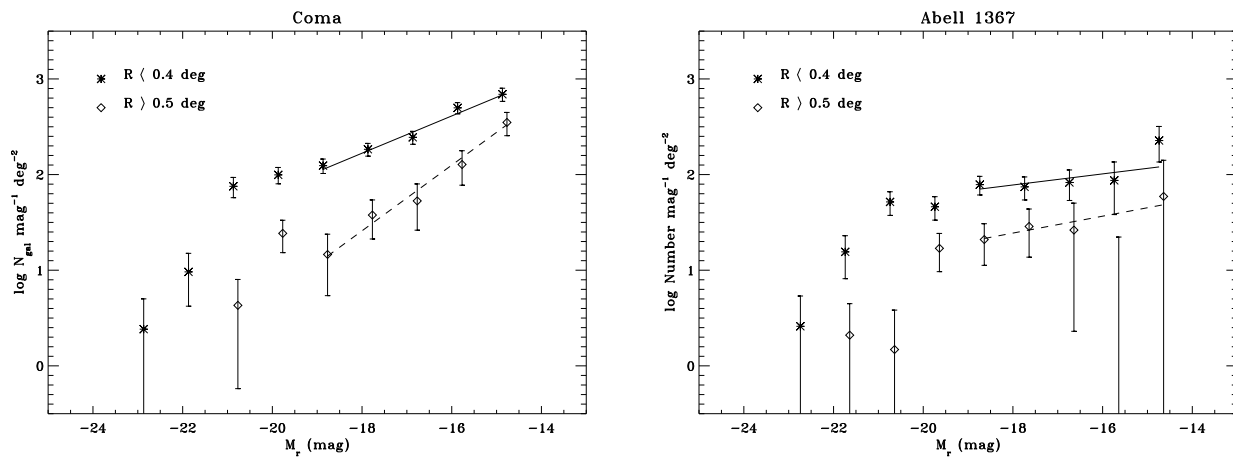


Fig. 8. Sloan r' -band LFs for the inner and outer regions of Abell 1367 (left plot) and Coma (right plot).

Appendix A: Overview of the Catalogs

Name	hh	mm	ss	dd	md	sd	r'	$\Delta r'$	$\mu_{25.5}$	$\Delta\mu_{25.5}$	Area	God	θ	Ellip.	S/G
	(J2000.)			(J2000.)			(mag)		(mag arcsec ⁻²)		arcsec ²		(deg.)		
113957+194339	11	39	57.8	19	43	39	20.68	0.02	23.88	0.02	17.96	0	174.59	0.44	0.53
113958+195514	11	39	58.4	19	55	14	20.08	0.01	23.80	0.02	27.72	0	157.09	0.07	0.07
113958+194515	11	39	58.5	19	45	15	19.88	0.01	23.64	0.02	32.16	0	69.50	0.15	0.03
113958+194329	11	39	58.7	19	43	29	20.84	0.02	23.84	0.02	14.30	0	72.89	0.20	0.47
113958+194333	11	39	58.8	19	43	33	19.32	0.01	23.48	0.02	41.14	0	162.66	0.05	0.03
113958+194827	11	39	58.8	19	48	27	17.79	0.00	22.99	0.01	111.89	0	139.41	0.44	0.03
113958+194702	11	39	58.8	19	47	2	20.87	0.02	24.06	0.03	17.52	0	55.84	0.33	0.01
113958+200102	11	39	58.9	20	1	2	19.26	0.01	23.46	0.02	43.25	0	19.05	0.25	0.03
113958+195339	11	39	59.0	19	53	39	19.72	0.01	23.43	0.02	27.39	0	54.46	0.05	0.29
113959+194251	11	39	59.1	19	42	51	20.21	0.02	24.00	0.02	26.17	0	62.95	0.41	0.16
113959+195403	11	39	59.1	19	54	3	20.58	0.02	24.14	0.03	23.40	0	164.80	0.18	0.02
113959+194743	11	39	59.3	19	47	43	20.94	0.02	24.04	0.02	13.42	0	104.87	0.13	0.63
113959+194703	11	39	59.3	19	47	3	20.52	0.02	24.06	0.03	22.40	0	137.74	0.25	0.03
113959+194700	11	39	59.6	19	47	0	20.43	0.01	23.97	0.02	22.51	0	116.33	0.20	0.03
113959+194948	11	39	59.8	19	49	48	20.24	0.01	23.95	0.02	26.17	0	26.36	0.22	0.02
113959+195210	11	39	59.8	19	52	10	19.40	0.01	23.45	0.02	38.70	0	95.13	0.05	0.20
113959+195346	11	39	59.8	19	53	46	20.92	0.02	24.12	0.03	16.19	0	25.87	0.11	0.37
113959+195456	11	39	59.9	19	54	56	19.87	0.01	23.54	0.02	26.17	0	70.95	0.20	0.13
114000+194327	11	40	0.1	19	43	27	18.82	0.01	23.41	0.01	61.77	0	118.40	0.20	0.03
114000+195714	11	40	0.2	19	57	14	19.96	0.01	23.68	0.02	27.61	0	27.04	0.07	0.07
114000+195343	11	40	0.3	19	53	43	17.42	0.00	22.97	0.01	155.24	0	164.95	0.23	0.08
114000+194340	11	40	0.5	19	43	40	19.92	0.01	23.78	0.02	30.38	0	38.22	0.10	0.05
114000+195426	11	40	0.6	19	54	26	15.63	0.00	22.39	0.01	462.96	0	152.53	0.20	0.03
114000+195048	11	40	0.7	19	50	48	18.93	0.01	23.08	0.01	41.81	0	57.56	0.26	0.10
114001+195315	11	40	1.1	19	53	15	20.60	0.02	23.83	0.02	16.52	0	29.89	0.07	0.12
114001+194401	11	40	1.2	19	44	1	18.84	0.01	23.12	0.01	47.02	0	102.02	0.17	0.04
114001+195729	11	40	1.3	19	57	29	19.18	0.01	23.22	0.01	37.48	0	109.11	0.14	0.04
114001+195330	11	40	1.3	19	53	30	20.00	0.01	24.07	0.03	36.15	0	80.50	0.26	0.02
114001+194355	11	40	1.3	19	43	55	19.30	0.01	23.48	0.02	41.81	0	149.09	0.20	0.06
114001+200001	11	40	1.4	20	0	1	19.67	0.01	24.44	0.03	55.56	0	6.00	0.23	0.00
114001+195821	11	40	1.7	19	58	21	19.77	0.01	23.72	0.02	33.16	0	114.59	0.32	0.03
114002+195313	11	40	2.4	19	53	13	19.36	0.01	23.32	0.01	35.15	0	86.57	0.17	0.03
114002+195324	11	40	2.5	19	53	24	20.39	0.01	23.81	0.02	20.85	0	58.13	0.16	0.05
114002+194219	11	40	2.5	19	42	19	20.43	0.01	23.99	0.02	22.95	0	26.57	0.11	0.03
114002+194331	11	40	2.7	19	43	31	19.02	0.01	23.34	0.01	49.57	0	49.21	0.10	0.03
114002+200227	11	40	2.7	20	2	27	20.89	0.03	24.38	0.03	16.08	0	125.59	0.18	0.04
114002+194931	11	40	2.9	19	49	31	18.27	0.01	23.24	0.01	89.93	0	9.50	0.16	0.03
114002+194212	11	40	3.0	19	42	12	17.33	0.00	23.08	0.01	185.18	0	163.54	0.01	0.03
114003+195245	11	40	3.2	19	52	45	20.12	0.01	23.67	0.02	24.84	0	70.51	0.29	0.03
114003+194603	11	40	3.4	19	46	3	20.35	0.01	23.94	0.02	23.51	0	54.08	0.17	0.03
114003+200148	11	40	3.7	20	1	48	19.74	0.01	23.60	0.02	28.05	0	123.35	0.20	0.70
114003+194354	11	40	3.7	19	43	54	19.80	0.01	23.71	0.02	32.82	0	94.62	0.23	0.03
114003+200010	11	40	3.9	20	0	10	20.12	0.01	23.94	0.02	30.83	0	20.88	0.19	0.04
114003+195325	11	40	4.0	19	53	25	20.65	0.02	24.34	0.03	24.51	0	20.58	0.46	0.01
114004+195129	11	40	4.1	19	51	29	20.12	0.01	23.73	0.02	24.84	0	56.35	0.11	0.04
114004+195808	11	40	4.3	19	58	8	20.59	0.02	23.92	0.02	18.19	0	83.01	0.20	0.42
114004+194900	11	40	4.4	19	49	0	20.54	0.02	23.81	0.02	18.07	0	64.56	0.08	0.62
114004+194414	11	40	4.5	19	44	14	18.83	0.01	23.07	0.01	45.80	0	41.12	0.06	0.04
114004+195552	11	40	4.7	19	55	52	19.73	0.01	23.59	0.02	32.60	0	66.50	0.17	0.03
114004+194522	11	40	4.8	19	45	22	18.99	0.01	23.66	0.02	66.31	0	78.35	0.28	0.03
114005+195754	11	40	5.2	19	57	54	19.77	0.01	23.49	0.02	27.83	0	135.47	0.07	0.41
114005+194544	11	40	5.6	19	45	44	19.73	0.01	23.70	0.02	34.71	0	47.48	0.11	0.05
114005+200220	11	40	5.6	20	2	20	20.31	0.02	24.03	0.03	26.84	0	77.06	0.11	0.02
114006+200151	11	40	6.1	20	1	51	20.34	0.02	24.19	0.03	30.05	0	52.99	0.12	0.01
114006+200216	11	40	6.2	20	2	16	20.61	0.02	23.89	0.02	17.96	0	47.88	0.09	0.32